ELSEVIER

Free vibration of higher-order sandwich and composite arches, Part I: Formulation

Sudhakar R. Marur[a,*], Tarun Kant[b]

[a]CSS Foundation, 313, A4 Wing, Cauvery Block, NGH Complex, Koramangala, Bangalore 560047, India
[b]Department of Civil Engineering, Indian Institute of Technology, Powai, Mumbai 400076, India

Abstract

A higher-order refined model with seven degrees of freedom per node is presented in this paper for the free vibration analysis of composite and sandwich arches. The strain field is modeled through cubic axial, cubic transverse shear and linear transverse normal strain components. As the cross-sectional warping is accurately modeled by this theory, it does not require any shear correction factor. The stress–strain relationship is derived from an orthotropic lamina in a three-dimensional state of stress. The proposed higher-order formulation is validated, in this first part, through arches with various curvatures, aspect ratios, boundary conditions and materials.
© 2007 Elsevier Ltd. All rights reserved.

1. Introduction

Laminated composite and sandwich arches or curved beams are being used in various automotive, aero space, energy, medical and sports applications, to name a few, due to their high strength to weight ratio. Developing predictive capabilities to assess their vibration characteristics, *a priori*, is a key aspect of design of components with such materials.

Ahmed [1] evaluated the vibration characteristics of curved sandwich beams using finite elements with three to five degrees of freedom per node. He studied effects of factors such as core–face density ratio, core rigidity, core–face thickness and subtended angle on the arch frequency. Similarly, Petyt and Fleischer [2] adopted finite element models for the radial vibrations of a curved beam. They ascertained the role of subtended angle on the frequencies, for various end conditions. Veletsos et al. [3] studied the free vibrations of circular arches in their own plane and their mode shapes, through an iterative numerical procedure. Based on the modal and strain energy distribution patterns, they classified modes as flexural, axial or coupled. They extended their study later [4] by including rotatory inertia and shear deformation.

---

*Corresponding author.

E-mail addresses: srmarur@iitbombay.org (S.R. Marur), tkant@civil.iitb.ac.in (T. Kant).

Singh and Singh [5] studied the in plane vibrations of rotating rings and sectors, with shear deformation through finite element method. Balasubramanian and Prathap [6] explored the locking and field-consistency aspects of a shear flexible curved beam element for the vibration of stepped arches.

Heppler [7] developed Timoshenko beam elements, using trigonometric basis functions, for studying the vibration of curved beams. Qatu [8,9] developed an exact as well as Ritz method-based approximate solutions for the vibration of laminated composite arches. His book [10] elaborates the theoretical basis of composite arch vibrations, in detail.

Auciello and De Rosa [11] studied the vibrations of classical arches through Galerkin, Ritz and finite element methods. They examined the influence of cross-sectional variations and of flexible supports on the vibration of arches. Krishnan and Suresh [12] developed a cubic element to study the effects of curvature, shear deformation and rotary inertia on the fundamental frequency of curved beams. Krishnan et al. [13] explored the role of subtended angle on the fundamental frequency of arches, with various end conditions. Sakiyama et al. [14] studied the free vibrations of sandwich arches with elastic or visco elastic core, various axis shapes and end conditions, through Green functions. Tseng et al. [15,16] studied the vibrations of first-order shear deformable arches with variable curvature, using dynamic stiffness method. Kang et al. [17,18] studied the vibrations of shear deformable circular arches using differential quadrature method. Many authors [19–22] explored the influence of axial extension, rotatory inertia and shear deformation on the vibrations of arches, in the past.

Khdeir and Reddy [23] developed a third-order theory for the vibration studies of shallow composite arches. Raveendranath et al. studied the performance of a curved beam element with coupled polynomial distributions [24] and also developed a two-noded shear deformable curved element [25] for arch vibrations. Patel et al. [26] developed a B-spline-based curved element for vibration analysis of composite structures.

It can be observed from these studies, that the arch vibration problem had been studied either through classical theory or first-order shear deformable theory of Timoshenko [27]. Also, most of the reported work had been on cross-ply configuration.

The classical theory would be adequate only for thin sections. While the first-order theory can handle deeper sections, it has serious limitations such as the need for a shear correction factor [28], inability to model the cross-sectional warping—a key factor for sandwich constructions with stiff facings and weak cores. Also, it cannot model the variation of transverse displacement across the thickness or in other words the transverse normal strain. The third-order theory, though more realistic, has been solved through analytical solutions.

Thus, one can see the need for a theory capable of accurately modeling and analyzing deep composite and sandwich arches. This paper presents a higher-order formulation, precisely fulfilling that need.

This higher-order theory models the cross-sectional warping through cubic axial strain. It considers the variation of transverse displacement across the thickness through a linearly varying transverse normal strain. Also, it incorporates transverse shear strain, varying cubically across the cross-section. This theory does not require any shear correction factor and employs standard isoparametric elements. Its elasticity matrix had been derived, from an orthotropic lamina assumed to be in a three-dimensional state of stress, in such a way that even angle ply laminations can be studied using one-dimensional elements.

Through the free vibration analyses of shallow to deep and thin to thick laminated arches with various boundary conditions, the proposed higher-order formulation is validated in this paper.

2. Theoretical formulation

The higher-order displacement model, based on Taylor's series expansion [29], can be expressed, for an arch, as follows (Fig. 1):

$$u = u_0 + z\theta_x + z^2 u_0^* + z^3 \theta_x^*, \tag{1}$$

$$w = w_0 + z\theta_z + z^2 w_0^*, \tag{2}$$

where z is the distance from the neutral axis to any point of interest along the depth of the arch, u_0 and w_0 are axial and transverse displacements in x–z plane, θ_x is the face rotation about y-axis and u_0^*, θ_x^*, θ_z, w_0^* are the higher-order terms arising out of Taylor's series expansion and defined at the neutral axis.
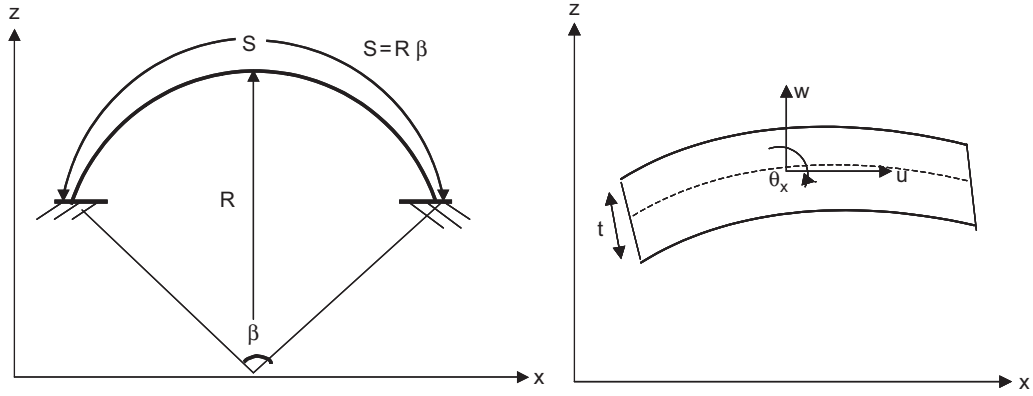
Fig. 1. Arch geometry with displacement components.

The Lagrangian function, in the absence of external and damping forces can be given as

$$L = T - U, \tag{3}$$

where T is the kinetic energy and U is the internal strain energy. The same can be expressed as

$$L = \frac{1}{2} \int \dot{\underset{\sim}{u}}^{\mathrm{t}} \rho \, \dot{\underset{\sim}{u}} \, \mathrm{d}v - \frac{1}{2} \int \varepsilon^{\mathrm{t}} \sigma \, \mathrm{d}v, \tag{4}$$

where

$$\underset{\sim}{u} = [u \; w]^{\mathrm{t}}, \; \dot{\underset{\sim}{u}} = [\dot{u} \; \dot{w}]^{\mathrm{t}}, \; \varepsilon = [\varepsilon_x \; \varepsilon_z \; \gamma_{xz}]^{\mathrm{t}}, \; \sigma = [\sigma_x \; \sigma_z \; \tau_{xz}]^{\mathrm{t}}. \tag{4a}$$

The field variables can be expressed in terms of nodal degrees of freedom as

$$\underset{\sim}{u} = Z_d d, \tag{5}$$

where

$$d = [u_0 \quad w_0 \quad \theta_x \quad u_0^* \quad \theta_x^* \quad \theta_z \quad w_0^*]^{\mathrm{t}}, \tag{5a}$$

$$Z_d = \begin{bmatrix} 1 & 0 & z & z^2 & z^3 & 0 & 0 \\ 0 & 1 & 0 & 0 & 0 & z & z^2 \end{bmatrix}. \tag{5b}$$

The strain field for an arch [10,16] can be expressed as

$$\varepsilon_x = \frac{1}{(1 + z/R)} (u_{,x} + w/R), \tag{6a}$$

$$\varepsilon_z = w_{,z}, \tag{6b}$$

$$\gamma_{xz} = w_{,x} + u_{,z} - u/R, \tag{6c}$$

where R is the radius of curvature.

Applying the displacement field from Eqs. (1) and (2) in the above equations, one gets

$$\varepsilon_x = \varepsilon_{x0} + z^2 \varepsilon_{x0}^* + z\kappa_x + z^3 \kappa_x^*, \tag{7a}$$

$$\varepsilon_z = \varepsilon_{z0} + z\kappa_z, \tag{7b}$$

$$\gamma_{xz} = \phi + z^2 \phi^* + z\chi_{xz} + z^3 \chi_{xz}^* \tag{7c}$$

and can be expressed in matrix form as

$$\varepsilon_x = Z_a^t \varepsilon_a + Z_b^t \varepsilon_b, \tag{8}$$

$$\varepsilon_z = Z_t^t \varepsilon_t, \tag{9}$$

$$\gamma_{xz} = Z_s^t \gamma_s, \tag{10}$$

where

$$\varepsilon_a = [\varepsilon_{x0} \ \varepsilon_{x0}^*]^t = [(u_{0,x} + w_0/R) \ (u_{0,x}^* + w_0^*/R)]^t, \tag{11a}$$

$$\varepsilon_b = [\kappa_x \ \kappa_x^*]^t = [(\theta_{x,x} + \theta_z/R) \ (\theta_{x,x}^*)]^t, \tag{11b}$$

$$\varepsilon_t = [\varepsilon_{z0} \ \kappa_z]^t = [\theta_z \ 2w_0^*]^t, \tag{11c}$$

$$\begin{aligned}
\gamma_s &= [\phi \ \phi^* \ \chi_{xz} \ \chi_{xz}^*]^t \\
&= [(w_{0,x} + \theta_x - u_0/R) \ (w_{0,x}^* + 3\theta_x^* - u_0^*/R) \ (\theta_{z,x} + 2u_0^* - \theta_x/R) \ (-\theta_x^*/R)]^t,
\end{aligned} \tag{11d}$$

$$Z_a = \left[\frac{1}{(1+z/R)} \ \frac{z^2}{(1+z/R)} \right]^t, \tag{11e}$$

$$Z_b = \left[\frac{z}{(1+z/R)} \ \frac{z^3}{(1+z/R)} \right]^t, \tag{11f}$$

$$Z_t = [1 \ z]^t, \tag{11g}$$

$$Z_s = [1 \ z^2 \ z \ z^3]^t. \tag{11h}$$

The strains of Eqs. (8)–(10) can be rewritten in a combined matrix form as

$$\varepsilon = \bar{Z}\bar{\varepsilon}, \tag{12}$$

where

$$\bar{Z} = \left[\begin{array}{ccc|c} Z_a^t & Z_b^t & 0 & 0 \\ 0 & 0 & Z_t^t & 0 \\ \hline 0 & 0 & 0 & Z_s^t \end{array} \right], \tag{12a}$$

$$\bar{\varepsilon} = [\varepsilon_a \ \varepsilon_b \ \varepsilon_t \ \gamma_s]^t. \tag{12b}$$

The stress–strain relationship of an orthotropic lamina in a three-dimensional state of stress can be expressed as [30]

$$\sigma^o = Q\varepsilon^o, \tag{13}$$

where

$$\sigma^o = [\sigma_x, \ \sigma_y, \ \sigma_z, \ \tau_{xy}, \ \tau_{yz}, \ \tau_{xz}]^t, \tag{13a}$$

$$\varepsilon^o = [\varepsilon_x, \ \varepsilon_y, \ \varepsilon_z, \ \gamma_{xy}, \ \gamma_{yz}, \ \gamma_{xz}]^t \tag{13b}$$

and Q is given by Eqs. (A.17)–(A.29), in Appendix A.

By setting σ_y, τ_{xy}, τ_{yz} equal to zero in Eq. (13) and deriving the remaining stress components from the same equation [31], one gets the stress–strain relationship as

$$\sigma = C\varepsilon, \tag{14}$$

where

$$\sigma = [\sigma_x, \ \sigma_z, \ \tau_{xz}]^t, \tag{14a}$$

$$C = \begin{bmatrix} C_{11} & C_{12} & 0 \\ C_{21} & C_{22} & 0 \\ \hline 0 & 0 & C_{33} \end{bmatrix} \tag{14b}$$

and the expressions for various C matrix elements are given by Eqs. (B.1)–(B.6), in Appendix B.

The internal strain energy can be evaluated using Eqs. (12) and (14) as

$$U = \frac{1}{2} \int \varepsilon^t \sigma \, dv = \frac{1}{2} \int \bar{\varepsilon}^t \bar{D} \bar{\varepsilon} \, dx, \tag{15}$$

where

$$\bar{D} = b \int \bar{Z}^t C \bar{Z} \, dz \tag{15a}$$

$$= b \int \begin{bmatrix} Z_a C_{11} Z_a^t & Z_a C_{11} Z_b^t & Z_a C_{12} Z_t^t & 0 \\ Z_b C_{11} Z_a^t & Z_b C_{11} Z_b^t & Z_b C_{12} Z_t^t & 0 \\ Z_t C_{21} Z_a^t & Z_t C_{21} Z_b^t & Z_t C_{22} Z_t^t & 0 \\ \hline 0 & 0 & 0 & Z_s C_{33} Z_s^t \end{bmatrix} dz, \tag{15b}$$

$$= \begin{bmatrix} D_{aa} & D_{ab} & D_{at} & 0 \\ D_{ba} & D_{bb} & D_{bt} & 0 \\ D_{ta} & D_{tb} & D_{tt} & 0 \\ \hline 0 & 0 & 0 & D_{ss} \end{bmatrix} \tag{15c}$$

and the expansions of various D matrices are given by Eqs. (C.3)–(C.11), in Appendix C.

The kinetic energy can be expressed using Eq. (5) as

$$T = \frac{1}{2} \int (\dot{d}^t \bar{m} \dot{d}) \, dx, \tag{16}$$

where

$$\bar{m} = b \sum_{l=1}^{NL} \int (z_d^t \rho_l z_d) \, dz, \tag{17}$$

where ρ_l is the mass density of a layer and $\bar{m}$ is given by Eqn. (C.12) in Appendix C.

The Lagrangian function can be re-stated with Eqs. (15) and (16) as

$$L = \frac{1}{2} \int (\dot{d}^t \bar{m} \dot{d}) \, dx - \frac{1}{2} \int (\bar{\varepsilon}^t \bar{D} \bar{\varepsilon}) \, dx. \tag{18}$$

3. Finite element modeling

The displacements within an element can be expressed in terms of its nodal displacements in isoparametric formulations as

$$d = N a_e, \tag{19}$$

where a_e is a vector containing nodal displacement vectors of an element with n nodes and can be expressed as

$$a_e = [d_1^t, \ d_2^t, \ \ldots, \ d_n^t]^t. \tag{20}$$

Similarly, the strains with in an element can be written through Eqs (5a) and (12b) as

$$\bar{\varepsilon} = \begin{bmatrix} B_a \\ B_b \\ B_t \\ B_s \end{bmatrix} a_e = \bar{B}a_e, \tag{21}$$

where, for a given node n, the strain displacement matrix can be computed as

$$B_a = \begin{bmatrix} N_{,x} & N/R & 0 & 0 & 0 & 0 & 0 \\ 0 & 0 & 0 & N_{,x} & 0 & 0 & N/R \end{bmatrix}_n, \tag{22}$$

$$B_b = \begin{bmatrix} 0 & 0 & N_{,x} & 0 & 0 & N/R & 0 \\ 0 & 0 & 0 & 0 & N/R & 0 & 0 \end{bmatrix}_n, \tag{23}$$

$$B_t = \begin{bmatrix} 0 & 0 & 0 & 0 & 0 & N & 0 \\ 0 & 0 & 0 & 0 & 0 & 0 & 2N \end{bmatrix}_n, \tag{24}$$

$$B_s = \begin{bmatrix} -N/R & N_{,x} & N & 0 & 0 & 0 & 0 \\ 0 & 0 & 0 & -N/R & 3N & 0 & N_{,x} \\ 0 & 0 & -N/R & 2N & 0 & N_{,x} & 0 \\ 0 & 0 & 0 & 0 & -N/R & 0 & 0 \end{bmatrix}_n. \tag{25}$$

By substituting Eqs. (19) and (21) in Eq. (18), one gets

$$L = \frac{1}{2}\dot{a}_e^{\mathrm{t}} \int N^{\mathrm{t}}\bar{m}N \, \mathrm{d}x \dot{a}_e - \frac{1}{2}a_e^{\mathrm{t}} \int \bar{B}^{\mathrm{t}}\bar{D}\bar{B} \, \mathrm{d}x a_e. \tag{26}$$

Applying Hamilton's principle on L, we get the governing equation of motion as

$$M\ddot{d} + Kd = 0, \tag{27}$$

where

$$M = \int N^{\mathrm{t}}\bar{m}N \, \mathrm{d}x \tag{27a}$$

and

$$K = \int \bar{B}^{\mathrm{t}}\bar{D}\bar{B} \, \mathrm{d}x. \tag{27b}$$

This equation of motion can be solved by expressing the displacement vector as

$$d = \bar{d}\mathrm{e}^{\mathrm{i}\omega t} = \bar{d}(\cos \omega t + \mathrm{i} \sin \omega t), \tag{28}$$

where $\bar{d}$ is the modal vector and ω the natural frequency. Substituting Eq. (28) into Eq. (27), one gets

$$(K - \omega^2 M)\bar{d} = 0. \tag{29}$$

By solving Eq. (29), using standard eigenvalue solvers [32], after applying suitable boundary conditions, the natural frequencies and corresponding mode shapes are directly obtained.

4. Numerical experiments

Numerical experiments have been carried out to study the performance of the proposed higher-order model. This model is validated by comparing its results with those available in the literature. Details such as material properties, lamination scheme and end conditions of every problem solved, are given in Table 1.

Table 1
Data for numerical experiments

1.1. *Nomenclature*
S—arc length of the arch
t—thickness of cross-section
R—radius of curvature
S/t—aspect ratio
$\beta(= S/R)$—subtended angle of an arch

r—radius of gyration of beam cross-section: $\sqrt{\dfrac{I}{A}} = 0.2887t$

FNP—frequency normalizing parameter
BC—boundary condition

1.2. *Boundary conditions for different supports*

Support type	at $x = 0$	at $x = S$
Simply supported (SS)	$u_0 = u_0^* = 0$ $w_0 = \theta_z = w_0^* = 0$	$u_0 = u_0^* = 0$ $w_0 = \theta_z = w_0^* = 0$
Simply supported (SS1)	$u_0 = 0$ $w_0 = \theta_z = w_0^* = 0$	$u_0 = u_0^* = 0$ $w_0 = \theta_z = w_0^* = 0$
Roller–simply support (RS)	$w_0 = \theta_z = w_0^* = 0$	$u_0 = u_0^* = 0$ $w_0 = \theta_z = w_0^* = 0$
Clamped–clamped (CC)	$u_0 = u_0^* = \theta_x = \theta_x^* = 0$ $w_0 = \theta_z = w_0^* = 0$	$u_0 = u_0^* = \theta_x = \theta_x^* = 0$ $w_0 = \theta_z = w_0^* = 0$
Clamped–free (CF)	$u_0 = u_0^* = \theta_x = \theta_x^* = 0$ $w_0 = \theta_z = w_0^* = 0$	All free

1.3. *Material data*

No.	Details	Ref.
Data-1	$\dfrac{E_1}{E_2} = 15$, $E_2 = E_3$, $\dfrac{G_{12}}{E_2} = 0.5$, $\dfrac{G_{23}}{E_2} = 0.5$, $\dfrac{G_{13}}{E_2} = 0.5$ $v = 0.25$, $\rho = 1$, $b = 1$, $t = 1$ FNP : $S^2\sqrt{\dfrac{12\rho}{E_1 t^2}}$ Lamination scheme: 0/90 No. of elements: 30 cubic BC:RS	[26]
Data-2	$\dfrac{E_1}{E_2} = 15, 40$ S/R = 1.0 Rest are same as Data-1	[10]
Data-3	$E_1 = E_2 = E_3 = 17{,}850 \,\text{N/cm}^2$ $G_{12} = G_{23} = G_{13} = 7140 \,\text{N/cm}^2$ $R = 43.18 \,\text{cm}$ $S = 67.8270 \,\text{cm}$, $\beta = 90°$ Mass/unit length $= 29.57 \times 10^{-4} \,\text{N s}^2/\text{cm}^2$ $v = 0.25$, $b = 1 \,\text{cm}$ $\rho = 0.00049426 \,\text{N s}^2/\text{cm}^4$, $t = 5.9827 \,\text{cm}$ (for $R/r = 25$) $\rho = 0.002767856 \,\text{N s}^2/\text{cm}^4$, $t = 1.0683 \,\text{cm}$ (for $R/r = 140$) FNP : $S^2\sqrt{\dfrac{12\rho}{E_1 t^2}}$ No. of elements: 30 cubic	[6,24]

Table 1 (*continued*)

1.3. *Material data*

No.	Details	Ref.
	BC:SS	
Data-4		[9,25]
	$\frac{E_1}{E_2} = 15,\ E_2 = E_3,\ \frac{G_{12}}{E_2} = 0.6,\ \frac{G_{23}}{E_2} = 0.6,\ \frac{G_{13}}{E_2} = 0.6$	
	$v = 0.25,\ \rho = 1,\ b = 1,\ t = 1$	
	$S/t = 100$	
	Lamination scheme: 0/90	
	FNP : $S^2 \sqrt{\dfrac{12\rho}{E_1 t^2}}$	
	No. of elements: 15 cubic	
	BC:CC	
Data-5		[7,13]
	$E_1 = E_2 = E_3 = 3.04 \times 10^7\,\text{lb/in}^2$	
	$G_{12} = G_{23} = G_{13} = 1.16923 \times 10^7\,\text{lb/in}^2$	
	$R = 12\,\text{in}$	
	$v = 0.3$	
	$\rho = 0.02763\,\text{lb s}^2/\text{in}^4,\ b = 1\,\text{in},\ t = 0.25\,\text{in}$	
	No. of elements: 30 cubic	
	BC:SS1	
Data-6		[18]
	$\frac{E_1}{E_2} = 1,\ E_2 = E_3,\ \frac{G_{12}}{E_2} = 0.5,\ \frac{G_{23}}{E_2} = 0.5,\ \frac{G_{13}}{E_2} = 0.5$	
	$v = 0.25,\ \rho = 1,\ b = 1,\ t = 1$	
	$S = 20$	
	FNP : $R^2 \sqrt{\dfrac{12\rho}{E_1 t^2}}$	
	No. of elements: 15 cubic	
	BC: SS, CC	
Data-7		[1]
	$S = 28\,\text{in},\ R = 168.06$	
	Face sheet:	
	$E_x = E_y = E_z = 1.0 \times 10^7\,\text{lb/in}^2$	
	$v = 0.3$	
	$\rho = 2.5098 \times 10^{-4}\,\text{lb s}^2/\text{in}^4$	
	$b_f = 1\,\text{in}$	
	$t_f\ (\text{top, bot}) = 0.018\,\text{in}$	
	Core:	
	$G_{xy} = G_{yz} = G_{xz} = 12.0 \times 10^3\,\text{lb/in}^2$	
	$v = 0.3$	
	$\rho = 3.0717 \times 10^{-6}\,\text{lb s}^2/\text{in}^4$	
	$b_c = 1\,\text{in}$	
	$t_c = 0.5\,\text{in}$	
	No. of elements: 30 cubic	
	BC:SS, CC, CF	

A laminated cross-ply arch modeled by a spline function and first-order shear theory [26] is analyzed using the present higher-order model (Table 2). One can observe close agreement between the results of present formulation and of spline functions. When the subtended angle is 180°, the first mode of vibration is axial, which is not reported in Ref. [26]. The remaining flexural modes compare well between the two.

Next, a cross-ply arch with varying aspect ratios and orthotropy is studied (Table 3). Flexural frequencies of thicker as well as thinner sections, predicted by the present theory match quite well with those of Ref. [10].

Table 2
Normalized natural frequencies of cross-ply laminated arch (Data-1)

β (deg)	Mode	$S/t = 20$		$S/t = 100$	
		Ref. [26]	Present	Ref. [26]	Present
5.72958	1	4.6463	4.6558	4.6981	4.6927
	2	17.9626	18.0615	18.8138	18.7805
	3	38.4482	38.6491	42.339	42.1740
	4	64.5268	63.3820	75.2691	74.7454
57.2958	1	4.0568	3.7680	4.0422	3.7203
	2	17.6089	17.5318	18.1587	17.8247
	3	38.4293	38.7940	41.6581	41.3503
	4	64.8491	65.5431	74.4162	74.1199
180	1	–	0.1563(a)	–	0.0723 (a)
	2	12.7163	11.6498	12.743	11.6111
	3	34.2522	33.3266	36.0239	34.6083
	4	61.7930	61.2770	68.9281	67.4113

(a) Axial frequency.

Table 3
Normalized natural frequencies of cross-ply laminated arch (Data-2)

Flexural modes	$S/t = 5$		$S/t = 10$		$S/t = 20$		$S/t = 50$		$S/t = 100$	
	Ref. [10]	Present	Ref. [10]	Present	Ref. [10]	Present	Ref. [10]	Present	Ref. [10]	Present
$E1/E2 = 15$										
1	3.3312	3.5242	3.7419	3.7551	3.9109	3.7680	3.9885	3.7369	4.0094	3.7203
2	11.8080	12.5238	15.3290	16.1191	17.0890	17.5318	17.8390	17.8429	18.0000	17.8247
3	21.4810	22.1833	31.3000	32.4565	37.6670	38.7940	40.6810	41.1215	41.2860	41.3503
4	31.2950	31.8372	49.4520	50.8358	64.0410	65.5431	72.0950	73.0511	73.7380	74.1199
$E1/E2 = 40$										
1	2.5935	2.6735	3.0814	3.0938	3.2932	3.1891	3.3871	3.1834	3.4108	3.1703
2	8.3979	8.4724	11.9640	12.2814	14.1110	14.4203	15.0930	15.1237	15.2980	15.1708
3	14.4460	14.3109	23.1800	23.1838	30.2830	30.7355	35.2200	34.5691	35.0340	35.1184
4	20.4250	20.0287	35.1180	34.5143	50.0170	50.0287	60.1780	60.7508	62.4380	62.7629

A 90° isotropic arch with different R/r ratios is studied (Table 4) and results are compared with earlier investigations. In the case of deep arch, current results match well with those of a field consistent formulation incorporating shear deformation and rotatory inertia [6]. As the formulations of Veletsos et al. [3] and Raveendranath et al. [24] do not consider transverse shear, their systems are stiffer predicting higher frequencies than those of current higher-order model and Ref. [6], for deep sections. The fourth and fifth frequencies of higher-order model turn out to be coupled modes, wherein the axial and flexural displacements are predominant, as shown in Figs. 2 and 3, while the seventh mode is a pure axial mode (Fig. 4).

In the case of shallow and thin arches, the results of present model and those of Refs. [3,24] can be seen to be in good agreement, for all modes. It is interesting to see the fifth vibration mode of current model, which is flexural, where in the entire transverse displacement being on the positive y-axis (Fig. 5).

Another cross-ply clamped arch is analyzed for various internal angles—zero to Π radians (Table 5). For all the internal angles, close agreement between the present model and earlier works can be observed.

In Table 6, natural frequencies of a simply supported circular arch, reported by Heppler [7], Krishnan et al. [13] and Tufekci [19] are compared with those of present higher-order theory. One can observe that the

Table 4
Normalized natural frequencies of hinged circular arch (Data-3)

Mode	$R/r = 25$				$R/r = 140$			
	Ref. [24]	Ref. [3]	Ref. [6]	Present	Ref. [24]	Ref. [3]	Ref. [6]	Present
1	33.6	33.76	32.04	32.5483	33.95	33.96	33.88	33.8933
2	53.42	53.41	52.44	52.6887	79.73	79.65	79.36	79.3554
3	88.25	88	80.82	80.7580	152.68	152.1	151.96	151.0825
4	130.72	130.3	121.7	123.83 (c)	235.77	233.8	234.24	231.6069
5	160.28	158.9	144.22	142.28 (c)	338.44	337.6	338.39	336.8383
6	239.16	237.6	192.47	193.6482	355.52	349.3	360.86	344.1158
7	–	258.4	251.79	252.82 (a)	–	481.4	515.59	474.0753
8	–	348.9	266.95	262.0879	–	623.9	710.2	607.9076

(a) Axial frequency.
(c) Coupled mode.
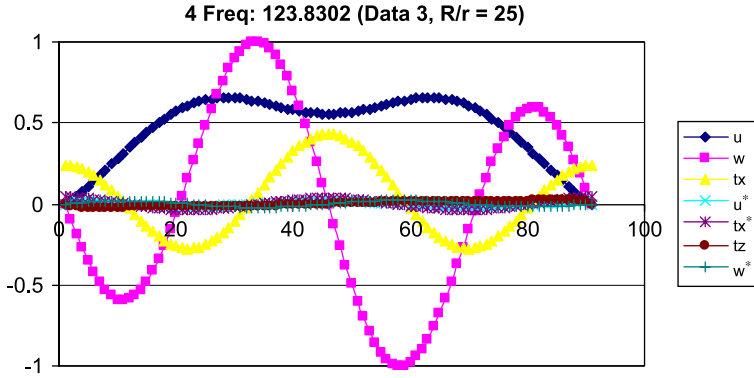
Fig. 2. Axial–flexural coupled mode.
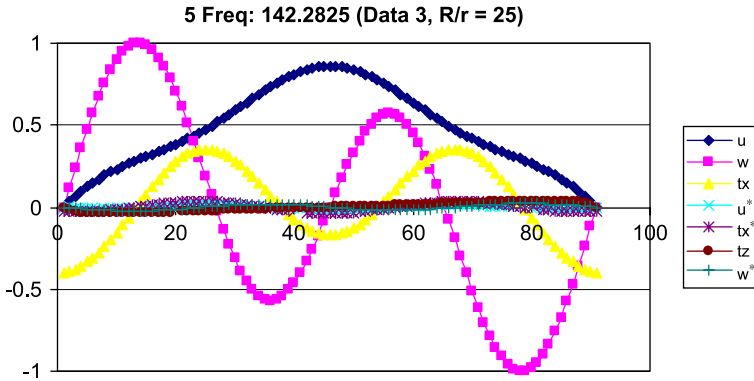
Fig. 3. Axial–flexural coupled mode.

prediction of the current formulation being quite closer to those of an exact solution [19] for the entire range of subtended angles. Similarly, close agreement between the finite element results [13] and the present theory can be seen, for the fundamental mode. However, the considerable difference between the results of Heppler [7] and the rest, at higher internal angles and in higher modes can be attributed [19] to the adoption of a constant number of (eight) straight beam elements to model the arch by Heppler. As the arc length increases with the increase in subtended angle, employing constant number of elements would be inadequate to model the arch
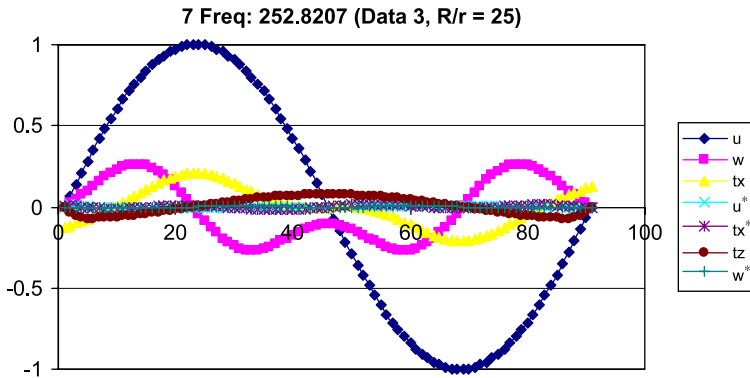
Fig. 4. Pure axial mode.
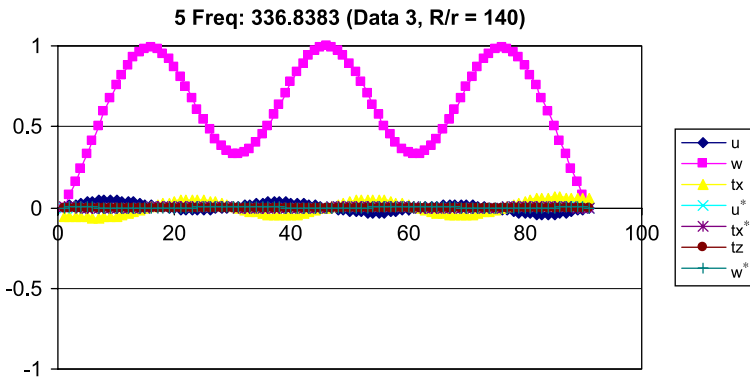
Fig. 5. Pure flexural mode.

Table 5
Normalized natural frequencies of cross-ply laminated arch (Data-4)

β	Ref. [25]	Ref. [9]	Present
Beam	10.66	10.661	10.6507
0.01	10.86	10.866	10.8559
0.02	11.46	11.459	11.4492
0.05	14.95	14.941	14.9364
0.1	23.33	23.265	23.2665
0.2	29.52	29.311	29.2704
0.3	29.47	29.236	29.2179
0.4	29.39	29.137	29.1409
0.5	29.3	29.015	29.0398
0.8	28.86	28.513	28.5972
1	28.46	28.074	28.1931
2	25.44	24.936	25.1595
3.14	20.94	20.441	20.6711

accurately, resulting in errors. It can be seen that the fundamental mode of vibration becomes axial, as the internal angle reaches 180° or more; for the rest it remains flexural. This is an ideal example for the validation of the current model, possibly for the widest range of internal angles from 10° to 350°.

Table 6
Natural frequencies (rad/s) of hinged circular arch (Data-5)

β (deg)		ω_1	ω_2	ω_3	ω_4
10	Ref. [7]	5849.90	19852.00	41173.00	50054.00
	Ref. [13]	5874.30	–	–	–
	Present	5770.90	19781.84	41003.16	47936.1 (a)
20	Ref. [7]	2830.20	5248.30	11642.00	20149.00
	Ref. [13]	2823.1	–	–	–
	Ref. [19]	2827.48	5246.73	11587.2	19825.8
	Present	2780.82	5225.06	11538.92	19762.23
30	Ref. [7]	2339.70	2528.30	5385.40	9438.10
	Ref. [13]	2345.20	–	–	–
	Present	2328.92	2495.36	5317.66	9161.29
60	Ref. [7]	560.24	1246.1	2456.7	2642.4
	Ref. [13]	561.2	–	–	–
	Ref. [19]	560.074	1226.61	2339.14	2627.75
	Present	557.60	1221.73	2329.03	2606.59
90	Ref. [7]	229.77	553.63	1102.30	1786.70
	Ref. [13]	230.4	–	–	–
	Ref. [19]	229.591	538.332	1024.89	1583.23
	Present	228.5753	536.0288	1020.37	1576.60
120	Ref. [7]	115.64	307.39	630.97	1060.80
	Ref. [13]	116.3	–	–	–
	Ref. [19]	115.609	291.549	562.463	887.37
	Present	115.0986	290.2717	559.9642	883.4933
150	Ref. [7]	64.44	196.66	422.55	732.19
	Ref. [13]	64.93	–	–	–
	Ref. [19]	64.4161	177.256	348.716	559.208
	Present	64.1331	176.4696	347.1570	556.7321
180	Ref. [7]	37.865	139.94	318.18	568.26
	Ref. [13]	38.24	–	–	–
	Ref. [19]	37.8485	115.541	233.152	380.269
	Present	37.684 (a)	115.0254	232.1072	378.5670
210	Ref. [7]	22.77	108.63	261.71	480.28
	Ref. [13]	23.05	–	–	–
	Ref. [19]	22.7629	78.7429	163.964	272.348
	Present	22.6663 (a)	78.3909	163.2276	271.1246
240	Ref. [7]	13.67	90.37	229.03	429.69
	Ref. [13]	13.87	–	–	–
	Ref. [19]	13.6592	55.252	119.464	202.425
	Present	13.604 (a)	55.0052	118.9269	201.5166
270	Ref. [7]	7.9246	79.1120	208.6300	398.2100
	Ref. [13]	8.06	–	–	–
	Ref. [19]	7.9204	39.5021	89.2883	154.649
	Present	7.8922 (a)	39.3263	88.8871	153.9523
300	Ref. [7]	4.1855	71.6810	194.7800	376.8200
	Ref. [13]	4.27	–	–	–
	Ref. [19]	4.184	28.5533	67.9828	120.633
	Present	4.1749 (a)	28.4273	67.6777	120.0914
330	Ref. [7]	1.6922	66.3930	184.5400	360.9000
	Ref. [13]	1.73	–	–	–
	Ref. [19]	1.6918	20.7348	52.4561	95.6193
	Present	1.701 (a)	20.6446	52.2222	95.1927

Table 6 (*continued*)

β (deg)		ω_1	ω_2	ω_3	ω_4
350	Ref. [7]	0.2440	63.5870	178.9000	352.1000
	Ref. [13]	0.5000	–	–	–
	Present	0.5354 (a)	16.6763	44.1700	82.1122

(a) Axial frequency.

Table 7
Normalized natural frequencies of clamped arch (Data-6)

β	SS		β	CC	
	Ref. [18]	Present		Ref. [18]	Present
pi/3	33.63	33.2042	Pi	4.3844	4.2466
pi/2	13.762	13.6061	13pi/10	2.1335	2.0715
pi	2.2669	2.2574	3pi/2	1.3948	1.3577
4pi/3	0.818	0.8235	9pi/5	0.7885	0.7713
3pi/2	0.4742	0.4837	2pi	0.5662	0.5563

Table 8
Natural frequencies (Hz) of sandwich arch (Data-7)

Mode	Ref. [1]	Ref. [33]	Ref. [14]	Present
CC				
1	264.2	240.0	244.6	243.2431
2	522.0	474.0	485.6	477.4111
3	889.0	843.0	859.8	839.3961
4	1312.0	1253.0	1276.0	1237.50
5	1767.0	1697.0	1725.0	1664.37
6	–	–	2190.0	2103.31
7	–	–	2668.0	2550.20
8	–	–	3151.0	2998.08

Mode	Ref. [1]	Ref. [14]	Present
SS			
1	199.5	182.7	182.2877
2	394.0	351.4	348.2241
3	746.0	726.1	714.3247
4	1175.0	1162.0	1135.0752
5	1639.0	1633.0	1585.4760
6	–	2118.0	2044.8443
7	–	2611.0	2506.7768
8	–	3104.0	2966.0851

Mode	Ref. [1]	Ref. [14]	Present
CF			
1	179.0	33.8	33.74
2	266.0	198.5	197.04
3	546.0	513.0	505.07
4	934.0	910.0	889.61
5	1379.0	1356.0	1317.20
6	–	1657.0	1655.70 (a)
7	–	1831.0	1768.83
8	–	2316.0	2225.18

(a) Axial frequency.

Another isotropic arch with SS and CC end conditions and various internal angles, up to 360°, is analyzed and compared with the results of ref. [18]. Close agreement between the two can be observed in Table 7.

Next, a sandwich arch analyzed earlier by Ahmed [1,33] and later by Sakiyama et al. [14] is studied using the present model (Table 8). As the first work of Ahmed [1] did not capture the transverse shear deformation, its frequency predictions have been quite high compared with other works, for all types of end conditions; while his subsequent work [33] on shear deformable sandwich beam agrees closely with the present model and Ref. [14], for clamped–clamped condition. The magnitude of frequencies of higher-order theory can be seen to be closer to those of first-order theory with a constant shear strain approximation [14], as the arch is a thin one with a S/t ratio of 52. As the current model employs additional higher-order degrees of freedom, it becomes more flexible than the rest.

These examples had been carefully chosen in order to capture the variation in curvature, aspect ratio and degree of orthotropy, on the vibration characteristics. The accuracy and adequacy of the higher-order model are validated, through the good agreement observed between the present model and the earlier works.

5. Conclusions

A higher-order model with transverse shear and normal strain components is formulated for studying the free vibrations of laminated arches. The proposed model can study shallow to deep and thin to thick arch geometries quite effectively. Through the constitutive relationship, adapted from the three-dimensional stress–strain relationship of an orthotropic lamina, even angle-ply laminates can be analyzed using one-dimensional elements. The proposed higher-order model is validated, in the first part of this paper, through the correlation of isotropic, orthotropic, composite and sandwich arch vibration characteristics with those of earlier investigations. In the second part of this paper, frequency spectrums of the higher-order model are identified and studied in greater detail.

Acknowledgments

Appendix A

The stress–strain relationship at a point of an orthotropic lamina in a three dimensional state of stress/strain can be expressed, along the lamina axes, as [30] (Fig. 6)

$$\sigma' = D\varepsilon', \tag{A.1}$$

where

$$\sigma' = \begin{bmatrix} \sigma_1 & \sigma_2 & \sigma_3 & \tau_{12} & \tau_{23} & \tau_{13} \end{bmatrix}, \tag{A.2}$$
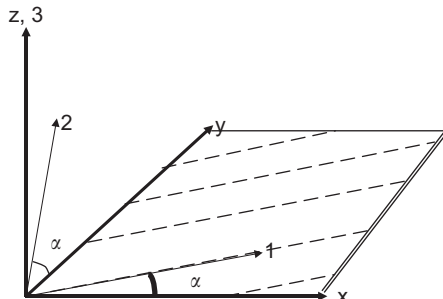

Fig. 6. x, y, z: laminate axes; $1, 2, 3$: lamina axes.

$$\varepsilon' = \begin{bmatrix} \varepsilon_1 & \varepsilon_2 & \varepsilon_3 & \gamma_{12} & \gamma_{23} & \gamma_{13} \end{bmatrix}, \tag{A.3}$$

$$D = \frac{1}{\Delta} \begin{bmatrix} E_1(1 - \nu_{23}\nu_{32}) & E_1(\nu_{21} + \nu_{31}\nu_{23}) & E_1(\nu_{31} + \nu_{21}\nu_{32}) & 0 & 0 & 0 \\ E_2(\nu_{12} + \nu_{13}\nu_{32}) & E_2(1 - \nu_{13}\nu_{31}) & E_2(\nu_{32} + \nu_{12}\nu_{31}) & 0 & 0 & 0 \\ E_3(\nu_{13} + \nu_{12}\nu_{23}) & E_3(\nu_{23} + \nu_{21}\nu_{13}) & E_3(1 - \nu_{12}\nu_{21}) & 0 & 0 & 0 \\ 0 & 0 & 0 & \Delta G_{12} & 0 & 0 \\ 0 & 0 & 0 & 0 & \Delta G_{23} & 0 \\ 0 & 0 & 0 & 0 & 0 & \Delta G_{13} \end{bmatrix}, \tag{A.4}$$

$$\Delta = (1 - \nu_{12}\nu_{21} - \nu_{23}\nu_{32} - \nu_{31}\nu_{13} - 2\nu_{12}\nu_{23}\nu_{31}). \tag{A.5}$$

The relation between engineering and tensor strain vectors, along lamina and laminate axes, can be given as

$$\varepsilon' = R\varepsilon'_{ts}, \tag{A.6}$$

$$\varepsilon^\circ = R\varepsilon^\circ_{ts}, \tag{A.7}$$

where

$$R = \begin{bmatrix} 1 & 0 & 0 & 0 & 0 & 0 \\ 0 & 1 & 0 & 0 & 0 & 0 \\ 0 & 0 & 1 & 0 & 0 & 0 \\ 0 & 0 & 0 & 2 & 0 & 0 \\ 0 & 0 & 0 & 0 & 2 & 0 \\ 0 & 0 & 0 & 0 & 0 & 2 \end{bmatrix}. \tag{A.8}$$

If the angle between lamina and laminate axes can be defined as α, then the lamina to laminate axis transformation is given by

$$T = \begin{bmatrix} c^2 & s^2 & 0 & 2sc & 0 & 0 \\ s^2 & c^2 & 0 & -2sc & 0 & 0 \\ 0 & 0 & 1 & 0 & 0 & 0 \\ -sc & sc & 0 & (c^2 - s^2) & 0 & 0 \\ 0 & 0 & 0 & 0 & c & -s \\ 0 & 0 & 0 & 0 & s & c \end{bmatrix}, \tag{A.9}$$

where

$$\begin{aligned} c &= \cos\alpha, \\ s &= \sin\alpha \end{aligned} \tag{A.10}$$

and the stress and strain along the lamina and laminate axes can be equated as

$$\sigma' = T\sigma^o, \tag{A.11}$$

$$\varepsilon'_{ts} = T\varepsilon^o_{ts}. \tag{A.12}$$

By making use of Eqs. (A.6)–(A.12), one can get the laminate stress–strain relationship as

$$\sigma^o = Q\varepsilon^o, \tag{A.13}$$

where

$$Q = T^{-1}D(T^{-1})^t, \tag{A.14}$$

$$(T^{-1})^t = RTR^{-1}, \tag{A.15}$$

$$Q = \begin{bmatrix} Q_{11} & Q_{12} & Q_{13} & Q_{14} & 0 & 0 \\ Q_{21} & Q_{22} & Q_{23} & Q_{24} & 0 & 0 \\ Q_{31} & Q_{32} & Q_{33} & Q_{34} & 0 & 0 \\ Q_{41} & Q_{42} & Q_{43} & Q_{44} & 0 & 0 \\ \hline 0 & 0 & 0 & 0 & Q_{55} & Q_{56} \\ 0 & 0 & 0 & 0 & Q_{65} & Q_{66} \end{bmatrix}, \tag{A.16}$$

$$Q_{11} = D_{11}c^4 + 2(D_{12} + 2D_{44})s^2c^2 + D_{22}s^4, \tag{A.17}$$

$$Q_{12} = D_{12}(s^4 + c^4) + (D_{11} + D_{22} - 4D_{44})s^2c^2, \tag{A.18}$$

$$Q_{13} = D_{31}c^2 + D_{32}s^2, \tag{A.19}$$

$$Q_{14} = (D_{11} - D_{12} - 2D_{44})sc^3 + (D_{12} - D_{22} + 2D_{44})s^3c, \tag{A.20}$$

$$Q_{22} = D_{11}s^4 + 2(D_{12} + 2D_{44})s^2c^2 + D_{22}c^4, \tag{A.21}$$

$$Q_{23} = D_{13}s^2 + D_{23}c^2, \tag{A.22}$$

$$Q_{24} = (D_{11} - D_{12} - 2D_{44})s^3c + (D_{12} - D_{22} + 2D_{44})sc^3, \tag{A.23}$$

$$Q_{33} = D_{33}, \tag{A.24}$$

$$Q_{34} = (D_{13} - D_{23})sc, \tag{A.25}$$

$$Q_{44} = (D_{11} - 2D_{12} + D_{22} - 2D_{44})s^2c^2 + D_{44}(c^4 + s^4), \tag{A.26}$$

$$Q_{55} = D_{55}c^2 + D_{66}s^2, \tag{A.27}$$

$$Q_{56} = (D_{66} - D_{55})sc, \tag{A.28}$$

$$Q_{66} = D_{55}s^2 + D_{66}c^2. \tag{A.29}$$

Appendix B

$$\Phi = (Q_{22}Q_{44} - Q_{24}^2), \tag{B.1}$$

$$C_{11} = Q_{11} + \frac{Q_{12}}{\Phi}(Q_{14}Q_{24} - Q_{12}Q_{44}) + \frac{Q_{14}}{\Phi}(Q_{12}Q_{24} - Q_{14}Q_{22}), \tag{B.2}$$

$$C_{12} = Q_{13} + \frac{Q_{12}}{\Phi}(Q_{24}Q_{34} - Q_{23}Q_{44}) + \frac{Q_{14}}{\Phi}(Q_{23}Q_{24} - Q_{22}Q_{34}), \tag{B.3}$$

$$C_{21} = Q_{13} + \frac{Q_{23}}{\Phi}(Q_{14}Q_{24} - Q_{12}Q_{44}) + \frac{Q_{34}}{\Phi}(Q_{12}Q_{24} - Q_{14}Q_{22}), \tag{B.4}$$

$$C_{22} = Q_{33} + \frac{Q_{23}}{\Phi}(Q_{24}Q_{34} - Q_{23}Q_{44}) + \frac{Q_{34}}{\Phi}(Q_{23}Q_{24} - Q_{22}Q_{34}), \tag{B.5}$$

$$C_{33} = Q_{66} - \frac{Q_{56}^2}{Q_{55}}. \tag{B.6}$$

Appendix C

Using Binomial series, the following terms can be expanded as

$$\frac{1}{(1+z/R)} = 1 - \frac{z}{R} + \frac{z^2}{R^2} - \frac{z^3}{R^3}, \tag{C.1}$$

$$\frac{1}{(1+z/R)^2} = 1 - \frac{2z}{R} + \frac{3z^2}{R^2} - \frac{4z^3}{R^3}, \tag{C.2}$$

which are used in the evaluation of various D matrices:

$$D_{aa} = b \int Z_a C_{11} Z_a^{\mathrm{t}}\, \mathrm{d}z = b \sum_{l=1}^{NL} C_{11} \left[\begin{array}{c|c} H_1 - \frac{2}{R}H_2 + \frac{3}{R^2}H_3 - \frac{4}{R^3}H_4 & H_3 - \frac{2}{R}H_4 + \frac{3}{R^2}H_5 - \frac{4}{R^3}H_6 \\[4pt] H_3 - \frac{2}{R}H_4 + \frac{3}{R^2}H_5 - \frac{4}{R^3}H_6 & H_5 - \frac{2}{R}H_6 + \frac{3}{R^2}H_7 - \frac{4}{R^3}H_8 \end{array} \right], \tag{C.3}$$

$$D_{ab} = b \int Z_a C_{11} Z_b^{\mathrm{t}}\, \mathrm{d}z = b \sum_{l=1}^{NL} C_{11} \left[\begin{array}{c|c} H_2 - \frac{2}{R}H_3 + \frac{3}{R^2}H_4 - \frac{4}{R^3}H_5 & H_4 - \frac{2}{R}H_5 + \frac{3}{R^2}H_6 - \frac{4}{R^3}H_7 \\[4pt] H_4 - \frac{2}{R}H_5 + \frac{3}{R^2}H_6 - \frac{4}{R^3}H_7 & H_6 - \frac{2}{R}H_7 + \frac{3}{R^2}H_8 - \frac{4}{R^3}H_9 \end{array} \right], \tag{C.4}$$

$$D_{ba} = D_{ab},$$

$$D_{bb} = b \int Z_b C_{11} Z_b^{\mathrm{t}}\, \mathrm{d}z = b \sum_{l=1}^{NL} C_{11} \left[\begin{array}{c|c} H_3 - \frac{2}{R}H_4 + \frac{3}{R^2}H_5 - \frac{4}{R^3}H_6 & H_5 - \frac{2}{R}H_6 + \frac{3}{R^2}H_7 - \frac{4}{R^3}H_8 \\[4pt] H_5 - \frac{2}{R}H_6 + \frac{3}{R^2}H_7 - \frac{4}{R^3}H_8 & H_7 - \frac{2}{R}H_8 + \frac{3}{R^2}H_9 - \frac{4}{R^3}H_{10} \end{array} \right], \tag{C.5}$$

$$D_{at} = b \int Z_a C_{12} Z_t^{\mathrm{t}}\, \mathrm{d}z = b \sum_{l=1}^{NL} C_{12} \left[\begin{array}{c|c} H_1 - \frac{2}{R}H_2 + \frac{3}{R^2}H_3 - \frac{4}{R^3}H_4 & H_2 - \frac{2}{R}H_3 + \frac{3}{R^2}H_4 - \frac{4}{R^3}H_5 \\[4pt] H_3 - \frac{2}{R}H_4 + \frac{3}{R^2}H_5 - \frac{4}{R^3}H_6 & H_4 - \frac{2}{R}H_5 + \frac{3}{R^2}H_6 - \frac{4}{R^3}H_7 \end{array} \right], \tag{C.6}$$

$$D_{bt} = b \int Z_b C_{12} Z_t^{\mathrm{t}}\, \mathrm{d}z = b \sum_{l=1}^{NL} C_{12} \left[\begin{array}{c|c} H_2 - \frac{2}{R}H_3 + \frac{3}{R^2}H_4 - \frac{4}{R^3}H_5 & H_3 - \frac{2}{R}H_4 + \frac{3}{R^2}H_5 - \frac{4}{R^3}H_6 \\[4pt] H_4 - \frac{2}{R}H_5 + \frac{3}{R^2}H_6 - \frac{4}{R^3}H_7 & H_5 - \frac{2}{R}H_6 + \frac{3}{R^2}H_7 - \frac{4}{R^3}H_8 \end{array} \right], \tag{C.7}$$

$$D_{ta} = b \int Z_t C_{21} Z_a^{\mathrm{t}}\, \mathrm{d}z = b \sum_{l=1}^{NL} C_{21} \left[\begin{array}{c|c} H_1 - \frac{2}{R}H_2 + \frac{3}{R^2}H_3 - \frac{4}{R^3}H_4 & H_3 - \frac{2}{R}H_4 + \frac{3}{R^2}H_5 - \frac{4}{R^3}H_6 \\[4pt] H_2 - \frac{2}{R}H_3 + \frac{3}{R^2}H_4 - \frac{4}{R^3}H_5 & H_4 - \frac{2}{R}H_5 + \frac{3}{R^2}H_6 - \frac{4}{R^3}H_7 \end{array} \right], \tag{C.8}$$

$$D_{tb} = b \int Z_t C_{21} Z_b^{\mathrm{t}}\, \mathrm{d}z = b \sum_{l=1}^{NL} C_{21} \left[\begin{array}{c|c} H_2 - \frac{2}{R}H_3 + \frac{3}{R^2}H_4 - \frac{4}{R^3}H_5 & H_4 - \frac{2}{R}H_5 + \frac{3}{R^2}H_6 - \frac{4}{R^3}H_7 \\[4pt] H_3 - \frac{2}{R}H_4 + \frac{3}{R^2}H_5 - \frac{4}{R^3}H_6 & H_5 - \frac{2}{R}H_6 + \frac{3}{R^2}H_7 - \frac{4}{R^3}H_8 \end{array} \right], \tag{C.9}$$

$$D_{tt} = b \int Z_t C_{22} Z_t^{t}\, \mathrm{d}z = b \sum_{l=1}^{NL} C_{22} \left[\begin{array}{cc} H_1 & H_2 \\ H_2 & H_3 \end{array} \right], \tag{C.10}$$

$$D_{ss} = b \int Z_s C_{33} Z_s^{\mathrm{t}}\, \mathrm{d}z = b \sum_{l=1}^{NL} C_{33} \left[\begin{array}{cccc} H_1 & H_3 & H_2 & H_4 \\ & H_5 & H_4 & H_6 \\ & & H_3 & H_5 \\ \mathrm{Sym} & & & H_7 \end{array} \right], \tag{C.11}$$

$$\bar{m} = b \sum_{l=1}^{NL} \rho_l \begin{bmatrix} H_1 & 0 & H_2 & H_3 & H_4 & 0 & 0 \\ & H_1 & 0 & 0 & 0 & H_2 & H_3 \\ & & H_3 & H_4 & H_5 & 0 & 0 \\ & & & H_5 & H_6 & 0 & 0 \\ & & & & H_7 & 0 & 0 \\ & \text{Sym} & & & & H_3 & H_4 \\ & & & & & & H_5 \end{bmatrix}. \tag{C.12}$$

In Eqs. (C.3)–(C.12), for a given layer l,

$$H_k = \frac{1}{k}(h_l^k - h_{l-1}^k), \tag{C.13}$$

where NL is the total number of layers of a cross-section, k the constant varying from 1 to 10, h_l the distance from the neutral axis to the top of a layer, l, h_{l-1} the distance from the neutral axis to the top of layer $l-1$ or bottom of layer l.

References

[1] K.M. Ahmed, Free vibration of curved sandwich beams by the method of finite elements, *Journal of Sound and Vibration* 18 (1971) 61–74.
[2] M. Petyt, C.C. Fleischer, Free vibration of a curved beam, *Journal of Sound and Vibration* 18 (1971) 17–30.
[3] A.S. Veletsos, W.J. Austin, C.A.L. Pereira, S.J. Wung, Free in plane vibration of circular arches, *ASCE Journal of Engineering Mechanics Division* 98 (1972) 311–329.
[4] W.J. Austin, A.S. Veletsos, Free vibration of arches flexible in shear, *ASCE Journal of Engineering Mechanics Division* 99 (1973) 735–753.
[5] K. Singh, B.P. Singh, Finite element method for in plane vibrations of rotating Timoshenko rings and sectors, *International Journal for Numerical Methods in Engineering* 21 (1985) 1521–1533.
[6] T.S. Balasubramanian, G. Prathap, A field consistent higher-order curved beam element for static and dynamic analysis of stepped arches, *Computers & Structures* 33 (1989) 281–288.
[7] G.R. Heppler, An element for studying the vibration of unrestrained curved Timoshenko beams, *Journal of Sound and Vibration* 158 (1992) 387–404.
[8] M.S. Qatu, In plane vibration of slightly curved laminated composite beams, *Journal of Sound and Vibration* 159 (1992) 327–338.
[9] M.S. Qatu, A.A. Elsharkawy, Vibration of laminated composite arches with deep curvature and arbitrary boundaries, *Computers & Structures* 47 (1993) 305–311.
[10] M.S. Qatu, *Vibration of Laminated Shells and Plates*, Elsevier Ltd., Oxford, 2004.
[11] N.M. Auciello, M.A. De Rosa, Free vibrations of circular arches: a review, *Journal of Sound and Vibration* 176 (1994) 433–458.
[12] A. Krishnan, Y.J. Suresh, A simple cubic linear element for static and free vibration analyses of curved beams, *Computers & Structures* 68 (1998) 473–489.
[13] A. Krishnan, S. Dharmaraj, Y.J. Suresh, Free vibration studies of arches, *Journal of Sound and Vibration* 186 (1995) 856–863.
[14] T. Sakiyama, H. Matsuda, C. Morita, Free vibration analysis of sandwich arches with elastic or visco elastic core and various kinds of axis shape and boundary conditions, *Journal of Sound and Vibration* 203 (1997) 505–522.
[15] Y.P. Tseng, C.S. Huang, C.J. Lin, Dynamic stiffness analysis for in-plane vibrations of arches with variable curvature, *Journal of Sound and Vibration* 207 (1997) 15–31.
[16] Y.P. Tseng, C.S. Huang, M.S. Kao, In-plane vibration of laminated curved beams with variable curvature by dynamic stiffness analysis, *Composite Structures* 50 (2000) 103–114.
[17] K. Kang, C.W. Bert, A.G. Striz, Vibration analysis of shear deformable circular arches by the differential quadrature method, *Journal of Sound and Vibration* 181 (1995) 353–360.
[18] K. Kang, C.W. Bert, A.G. Striz, Vibration and buckling analysis of circular arches using DQM, *Computers & Structures* 60 (1996) 49–57.
[19] E. Tufekci, A. Arpaci, Exact solution of in-plane vibrations of circular arches with account taken of axial extension, transverse shear and rotatory inertia effects, *Journal of Sound and Vibration* 209 (1998) 845–856.
[20] V. Yildirim, Rotary inertia, axial and shear deformation effects on the in-plane natural frequencies of symmetric cross-ply laminated circular arches, *Journal of Sound and Vibration* 224 (1999) 575–589.
[21] V. Yildirim, Common effects of the rotary inertia and shear deformation on the out-of-plane natural frequencies of composite circular bars, *Composites Part B: Engineering* 32 (2001) 687–695.
[22] H. Matsunaga, Free vibration and stability of laminated composite circular arches subjected to initial axial stress, *Journal of Sound and Vibration* 271 (2004) 651–670.

[23] A.A. Khdeir, J.N. Reddy, Free and forced vibration of cross-ply laminated composite shallow arches, *International Journal of Solids and Structures* 34 (1997) 1217–1234.

[24] P. Raveendranath, G. Singh, B. Pradhan, Free vibration of arches using a curved beam element based on a coupled polynomial displacement field, *Computers & Structures* 78 (2000) 583–590.

[25] P. Raveendranath, G. Singh, B. Pradhan, Application of coupled polynomial displacement fields to laminated beam elements, *Computers & Structures* 78 (2000) 661–670.

[26] B.P. Patel, M. Ganapathi, J. Saravanan, Shear flexible field-consistent curved spline beam element for vibration analysis, *International Journal for Numerical Methods in Engineering* 46 (1999) 387–407.

[27] S.P. Timoshenko, On the correction for shear in differential equation for transverse vibrations of prismatic bars, *Philosophical Magazine Series* 41 (1921) 744–746.

[28] G.R. Cowper, The shear coefficient in Timoshenko beam theory, *ASME Journal of Applied Mechanics* 33 (1966) 335–340.

[29] K.H. Lo, R.M. Christensen, E.M. Wu, A higher-order theory of plate deformation—part1: homogenous plates, *ASME Journal of Applied Mechanics* 44 (1977) 663–668.

[30] R.M. Jones, *Mechanics of Composite Materials*, McGraw-Hill Kogakusha, Tokyo, 1975.

[31] R.U. Vinayak, G. Prathap, B.P. Naganarayana, Beam elements based on a higher-order theory—I. Formulation and analysis of performance, *Computers & Structures* 58 (1996) 775–789.

[32] K.J. Bathe, *Finite Element Procedures in Engineering Analysis*, Prentice-Hall, Englewood Cliffs, NJ, 1982.

[33] K.M. Ahmed, Dynamic analysis of sandwich beams, *Journal of Sound and Vibration* 21 (1972) 263–276.